Entry inhibition and modulation of pro-inflammatory immune response against Influenza A Virus by a recombinant truncated surfactant protein D

Mohammed N. Al-Ahdal[1*], Valarmathy Murugaiah[2], Praveen M. Varghese[2], Suhair M. Abozaid[1], Iram Saba[1], Ahmed Al-Qahtani[1], Ansar A. Pathan[2], Lubna Kouser[2,3], Beatrice Nal-Rogier[2], Uday Kishore[2]

[1]Department of Infection and Immunity, King Faisal Specialist Hospital and Research Centre, Riyadh, Saudi Arabia

[2]Biosciences, College of Health and Life Sciences, Brunel University London, Uxbridge UB8 3PH, United Kingdom

[3]Allergy & Clinical Immunology Inflammation, Repair and Development, Imperial College London, London SW7 2AZ, United Kingdom

*Corresponding Author: Prof. M. N. Al-Ahdal (ahdal@kfshrc.edu.sa)

Running Tittle: Recombinant human SP-D as an entry inhibitor of IAV

Keywords: Innate immunity; Influenza A Virus; Surfactant Protein D; Pseudotyped Lentiviral Particles; inflammation

Acknowledgement: This work is part of a project funded by the Biotechnology program of the King Abdulaziz City for Science and Technology (14-MED258-20) and approved by the Research Advisory Council of the King Faisal Specialist Hospital and Research Centre, Riyadh (2150031). We thank Maureene Delos Reyes and Hanan Shaarawi for secretarial and logistic assistance.

Abstract

Surfactant protein D (SP-D), a C-type collagen containing lectin (collectin), is expressed in the mucosal secretion of the lung and contribute to the innate host defence against a variety of pathogens, including influenza A virus (IAV). SP-D has been shown to inhibit haemagglutination activity and infectivity of IAV, in addition to reducing neuraminidase (NA) activity. SP-D exhibits a strong anti-IAV activity by virtue of its carbohydrate recognition domain (CRD) binding to carbohydrate pattern (N-linked mannosylated) on NA and hemagglutinin (HA) of the IAV. Here, we demonstrate that a recombinant fragment of human SP-D (rfhSP-D), containing homotrimeric neck and CRD regions, acts as an entry inhibitor of IAV and down-regulates M1 expression considerably in A549 cells infected with pH1N1 as well as H3N2 IAV strains at 2h treatment. In addition, rfhSP-D down-regulated mRNA levels of TNF-α, IFN-α, IFN-β, IL-6 and RANTES production, as judged by qPCR, particularly during the initial stage of IAV infection of A549 cell line. rfhSP-D also interfered with IAV infection of Madin-Darby canine kidney (MDCK) cells through HA1 binding, as confirmed by luciferase reporter assay and far western blotting. Furthermore, rfhSP-D was found to reduce luciferase reporter activity of MDCK cells transduced with H1+N1 pseudotyped lentiviral particles in a dose-dependent manner, where 50% of reduction was observed with 10 μg/ml rhfSP-D. Thus, binding of rfhSP-D to HA1 and reduction in luciferase reporter activity are suggestive of a critical role of rfhSP-D in mediating the inhibition of IAV infectivity and that of pesudotyped lentivirus as an entry inhibitor. Multiplex cytokine array revealed that rfhSP-D treatment of IAV challenged A549 cells led to a dramatic suppression of some of the key pro-inflammatory cytokines and chemokines in the virus challenged A549 cells. In the case of pH1N1, soluble factors such as TNF-α, IFN-α, IL-10, IL-12 (p40), VEGF, GM-CSF and eotaxin were considerably suppressed by rfhSP-D treatment at 24h. However, these suppressive effects of IL-10, VEGF, eotaxin and IL-12 (p40) were not so evident in the case of H3N2 strain at the secreted protein level, with the exception of TNF-α, IFN-α, and GM-CSF. These data seem to suggest that the extent of immunomodulatory effect of SP-D on host cells can vary considerably in a strain-specific manner. Thus, rfhSP-D treatment can downregulate pro-inflammatory milieu encouraged by IAV via aberrant inflammatory cell recruitment leading to cell death and other possible long term immune defects and lung damage.

Introduction

The innate immune system is composed of both cellular and humoral players to encounter invading pathogens. It is also an important component in the initiation and modulation of the adaptive immunity. To distinguish self from non-self-recognition, the innate immune system has evolved to recognise pathogen associated molecular patterns (PAMPS) through a number of pattern recognition receptors (PRRs), including Toll like receptors, and C-type lectin receptors. Collectins are collagenous lectins, representing a crucial group of calcium-dependent pattern recognition molecules present in pulmonary secretions and mammalian serum (1). They play a crucial role in first line host defence against a diverse range of pathogens by interacting with specific glycoconjugates and lipid moieties present on the surface of microorganisms. A significant number of *in vitro and in vivo* studies have focused on the immunomodulatory functions of lung collectins, human surfactant protein D (SP-D). Such collectin, SP-D is is primarily organised into four regions: a cysteine-linked N-terminal region involved in multimerization, a triple-helical collagen region composed of Gly-X-Y repeats, an α-helical, coiled-coil trimerizing neck region, and the C-terminal carbohydrate recognition domains (CRD) or C-type lectin domain (Kishore et al., 2006). Human SP-D is primarily synthesised by alveolar type II and Clara cells, in addition to being present in several extra-pulmonary tissues. SP-D triggers a range of anti-microbial defence mechanisms, including agglutination/aggregation, phagocytosis, and direct growth inhibition (Nayak et al., 2012). SP-D is also capable of controlling pulmonary inflammation including allergy and asthma, and thus, linking innate with adaptive immunity via modulation of dendritic cell maturation and functions, and polarisation of helper T cells (1).

The direct nature of interaction between SP-D and a number of viruses has been reported (2, 3), which often results in viral neutralisation and enhanced phagocytosis (4, 5). Anti-viral roles of SP-D during Influenza A virus (IAV) infection have been well-documented, principally by Hartshorn group. IAV is an enveloped RNA virus and a member of Orthomyxoviridae family that possess eight single stranded RNA segments with negative orientation. These RNA segments can encode up to 13 viral proteins, including two surface glycoproteins, an ion channel protein, nucleocapsid protein, structural scaffolding protein, a tripartite polymerase complex, two non-structural proteins, and three non-essential proteins (6). IAV is subtyped based on their surface glycoproteins, such as hemagglutinin (HA) and neuraminidase (NA); to date, there are 19 HA and 9 NA protein subtypes that have been well established. Both HA and NA play an important role in the host range, viral replication and

pathogenicity (7). Among the three genera of influenza viruses reported, infection by IAV is the most common and severe in humans, swine and avian species. It is also known to cause pandemic infections, being diverse in host specificity. IAV is considered as a major human respiratory pathogen following 1918 H1N1 influenza pandemic (Spanish Flu) (8), which is believed to have resulted in the zoonotic transmission of an avian virus to a human host and has rapidly dispersed (9).

Binding of IAV to target cells is mediated via the globular head of HA to sialic acid (SA) receptors present on the host cell surface (10, 11). IAV strains have adapted to human preferentially via binding with α (2–6) linkage of SA receptors (12). Following IAV-SA receptor interaction, virus particles are internalised via clathrin, resulting in clathrin-mediated endocytosis, or via caveolin/clathrin- independent mechanism (13, 14). Thus, acidic environment triggers M2 ion channel and transfers protons and potassium into the interior portion of the virion to dissociate M1 protein from the ribonucleoprotein (RNP) (15). Acidification also initiates HA-mediated conformational changes, which lead to viral fusion and RNPs release into the cytoplasm, further resulting in viral transcription and replication process. It is, therefore, suggested that SA and its linkage is crucial for the initiation of IAV infection of both epithelial and immune cells. Thus, inhibition of SA receptor binding or enzymatic switching of SA-mediated linkages can confer cell resistance, and/or alter susceptibility to IAV infection. Hence, cell surface SA is considered as an important primary receptor and determinant of IAV tropism, contributing to induction of immune responses as well as to viral pathogenesis.

It is crucial to understand molecular mechanisms of host defence against IAV in order to design novel anti-IAV strategies. SP-D binding to HA leads to a direct inhibition of cellular infection by preventing HA-SA receptor interaction (3). SP-D has been shown to bind HA mediated glycosylation sites, identified as β-type inhibitor of IAV. This interaction is calcium dependent, and binding of SP-D to NA inhibits the release of progeny virions from infected cells (16, 17). It has been reported that recombinant full-length porcine SP-D has a potent antiviral activity against a wide range of IAV by similar mechanisms, more than human SP-D due to structural differences like an additional loop in its CRD, an additional glycosylation site and an additional cysteine in the collagen domain (18). In this study, we have used a well- characterized recombinant homotrimeric fragment of human SP-D comprising neck and CRD region (rfhSP-D), and examined its ability to act as an entry inhibitor of IAV and pseudotype viral particles, and modulate subsequent immunological response *in vitro.*

Materials and Methods

Reagents

Viruses and Reagents

The A/England/195/2009 (pH1N1) and the A/Hong Kong/1774/99 (H3N2) strains were gifted by Wendy Barclay from the Imperial College, London and Leo Poon from the University of Hong Kong, respectively. The plasmids used to produce the H1+N1 pseudotyped lentiviral particles were obtained from Addgene. The pHIV-Luciferase plasmid was a gift from Bryan Welm (Addgene plasmid # 21375); psPAX2 was a gift from Didier Trono (Addgene plasmid # 12260), and VSVG was offered by Bob Weinberg (Addgene plasmid #8454). Monoclonal Anti-Influenza Virus H1 Hemagglutinin (HA), A/California/04/2009 (H1N1)pdm09, Clone 5C12 (produced in vitro), NR-42019 and Polyclonal Anti-Influenza Virus H3 Hemagglutinin (HA), A/Hong Kong/1/1968 (H3N2), (antiserum, Goat), NR-3118 were obtained through BEI Resources, NIAID, NIH, USA

Cell culture

Adenocarcinomic human alveolar basal epithelial cells A549, Madin Darby canine kidney (MDCK), and Human embryonic kidney (HEK) 293T cell lines were cultured in Dulbecco's Modified Eagle's Medium (DMEM) (Sigma-Aldrich), supplemented with 10% v/v Fetal Bovine Serum (FBS), 2mM L-glutamine, 100U/ml penicillin (Sigma-Aldrich), 100µg/ml streptomycin (Sigma-Aldrich) and 1mM sodium pyruvate (Sigma-Aldrich), and left to grow at 37°C in the presence of 5% v/v CO_2 for approximately 3 days before passaging. Since these cells were adherent, they were detached using 2 × Trypsin-EDTA (0.5%) (Fisher Scientific) for 10 minutes at 37°C. Cells were then centrifuged at 1200 rpm for 5 minutes, followed by re-suspension in complete DMEM with FBS, penicillin and streptomycin, as described above. To determine the cell count and viability, an equal volume of the cell suspension and Trypan Blue (0.4% w/v) (Fisher Scientific) solution were vortexed, followed by cell count using a haemocytometer with Neubauer rulings (Sigma-Aldrich). Cells were then re-suspended in complete DMEM medium for further use.

Purification of IAV strains

MDCK cells at 80-90% confluency were washed with sterile PBS twice before infection. Diluted pandemic A/H1N1 2009 (pH1N1) ($2x10^4$) or A/Hong Kong/1774/99 (H3N2)

155 (3.3×10^4) (600µl/flask) was transferred to the flask containing 20 ml of complete DMEM
156 medium, and incubated at 37°C for 1h. Unbound viruses were removed by washing three
157 times with sterile PBS. 25 ml of infection medium (DMEM with 1% Penicillin/Streptomycin,
158 0.3% Bovine Serum Albumin (BSA) and 1µg/ml of L-1-Tosylamide-2-phenylethyl
159 chloromethyl ketone (TPCK) - Trypsin (Sigma-Aldrich) was added to the flasks, and
160 incubated at 37°C for 3 days. The virus particles were then harvested via centrifugation of
161 the infectious medium at 3000 × g at 4°C for 15 minutes. The supernatant obtained was
162 centrifuged at 10,000 × g for 30 minutes at 4°C. 26 ml of supernatant was added slowly to
163 new Ultra-clear centrifuge tubes containing 30% w/v sucrose (8 ml/tube) (Sigma-Aldrich),
164 and centrifuged at 25,000 × g at 4°C for 90 minutes. The upper phase of the medium and the
165 sucrose phase were carefully removed; IAV particles at the bottom were re-suspended in
166 100µl of sterile PBS. Virus suspension (15 µl) was subsequently analysed by SDS-PAGE and
167 ELISA.

168 **Tissue Culture Infectious Dose 50% ($TCID_{50}$) assay**

169 Purified pH1N1 or H3N2 virus stocks were prepared with a starting dilution of 10^{-2} in
170 DMEM and 146µl of the diluted virus was added to all wells; uninfected MDCK cells were
171 used as a control. 46µl of pH1N1 or H3N2 was then serially diluted ($1/2\log_{10}$ up to 10^{-7}) and
172 incubated at 37°C for 1h in a microtiter plate. 1×10^5 MDCK cells, earlier trypsinised and re-
173 suspended in 2× infectious medium, were added to each well and incubated for 3 days at
174 37°C under 5% v/v CO_2 until cytopathic effect (CPE) was observed. After 5 days, each well
175 was observed under microscopy, and the number of wells that were positive and negative for
176 CPE at each dilution was recorded.

177 **Expression and purification of a recombinant fragment of human SP-D containing neck**
178 **and CRD regions**

179 A recombinant fragment of human SP-D (rfhSP-D) was expressed under bacteriophage T7
180 promoter in *Escherichia coli* BL21 (λDE3) pLysS (Invitrogen), transformed with plasmid
181 pUK-D1 containing cDNA sequences for the 8 Gly-X-Y repeats, neck and CRD regions of
182 human SP-D, as described previously (19). Briefly, a primary inoculum of 25 ml bacterial
183 culture was inoculated into 500 ml of LB containing 100 µg/ml ampicillin and 34 µg/ml
184 chloramphenicol (Sigma-Aldrich), grown to OD_{600} of 0.6, and then induced with 0.5 mM
185 Isopropyl β-D-1-thiogalactopyranoside (IPTG) (Sigma-Aldrich) for 3 hours. The bacterial
186 cell pellet was re-suspended in lysis buffer (50 mM Tris-HCl pH7.5, 200 mM NaCl, 5 mM

EDTA pH 8, 0.1% v/v Triton X-100, 0.1mM phenyl-methyl-sulfonyl fluoride (PMSF), 50 μg/ml lysozyme) and sonicated (five cycles, 30 seconds each). The sonicate was harvested at 12000 × g for 30 minutes, followed by solubilisation of inclusion bodies in refolding buffer (50 mM Tris-HCl pH 7.5, 100 mM NaCl, 10 mM 2-Mercaptoethanol) containing 8M urea. The solubilised fraction was then dialysed stepwise against refolding buffer containing 4 M, 2 M, 1 M and no urea. The clear dialysate was loaded onto a maltose agarose column (5 ml; Sigma-Aldrich) and the bound rfhSP-D was eluted using 50 mM Tris-HCl, pH 7.5, 100 mM NaCl and 10 mM EDTA. The eluted fractions were then passed through PierceTM High Capacity Endotoxin Removal Resin (Qiagen) to remove endotoxin. The endotoxin levels were measured via QCL-1000 Limulus amebocyte lysate system (Lonza), and found to be < 5pg/ μg of rfhSP-D.

Direct binding ELISA

Maxisorp 96 well microtiter plates were coated with rfhSP-D (5, 2.5, 1.25, 0.625 μg/well) in carbonate-bicarbonate buffer (CBC), pH 9.6, and incubated overnight at 4°C. After removing the coating buffer, microtiter wells were washed with PBS three times, blocked with 2% w/v BSA in PBS for 2h at 37°C, and then washed three times with PBST (PBS + 0.05% Tween 20). 20 μl of concentrated pH1N1, H3N2 virus (1.36×10^6 pfu/ml), or purified recombinant HA (2.5 μg/ml) was diluted in 200 μl of PBS, 10 μl of diluted virus was added to each wells, and incubated at RT for 2h in buffer containing 5mM $CaCl_2$. Vesicular stomatitis Indiana virus (VSVG) (Addgene) lentivirus was used as a negative control. The microtiter wells were washed with PBST three times and the binding was probed with primary antibody: monoclonal anti-influenza virus H1 (BEI-Resources) and polyclonal anti-influenza virus H3 (BEI-Resources) antibody (1:5000 dilution in PBS) for 1 hour at 37°C. The wells were washed again with PBST and incubated with anti-mouse IgG-Horseradish peroxidase (HRP)-conjugate (1:5000) (Fisher Scientific) and Protein A-HRP-conjugate (Fisher Scientific) in PBS (100μl/well), respectively, for 1h at 37°C. Colour was developed using 3,3',5,5'-Tetramethylbenzidine (TMB) substrate (Sigma-Aldrich). The reaction was stopped using 2N H_2SO_4 and the absorbance was read at 450nm using iMark™ microplate absorbance reader (Bio-Rad).

Far western blotting

rfhSP-D (5μg) or 10 μl of concentrated pH1N1/H3N2 (1.36×10^6pfu/ml) were run separately on a 12% (w/v) SDS-PAGE, and then electrophoretically transferred onto a nitrocellulose

membrane (320 mA for 2h) in 1× transfer buffer (25 mM Tris-HCl pH 7.5, 190 mM glycine and 20% methanol), followed by blocking overnight in 5% w/v dried milk powder in PBS (Sigma-Aldrich) at 4 °C on a rotatory shaker. The membrane was then washed with PBST three times, 10 minutes each. For far western blotting, the nitrocellulose membrane was incubated with 5µg/ml of rfhSP-D in PBS containing 5mM $CaCl_2$ for 1h at room temperature (RT) and 1h at 4°C. Following PBST wash, the membrane was incubated with primary antibodies, polyclonal rabbit anti-human SP-D, monoclonal anti-influenza virus H1 (BEI-Resources), or polyclonal anti-influenza virus H3 (BEI-Resources) in PBS (1:1000) for 1h at RT. Following washing, the membrane was probed with secondary antibodies: Protein-A-HRP-conjugate, or rabbit anti-mouse IgG HRP conjugate (1:1000) (Fisher Scientific) in PBS (100µl/well) for 1h at RT. After PBST wash, the blot was developed either using 3,3'-diaminobenzidine (DAB) or enhanced chemiluminescence (ECL) substrate. For M1 detection, following 6h incubation, both untreated (cells +virus) and treated samples (cells+ virus + 10µg/ml rfhSP-D) were run on the 12% (w/v) SDS-PAGE, and transferred onto a nitrocellulose membrane, as described above. The M1 expression was detected using Anti-M1 monoclonal antibody (BEI-Resources).

Cell binding assay

A549 cells were seeded in microtiter wells using DMEM complete medium (1×10^5 cells/well) and incubated overnight at 37°C. The wells were washed with PBS three times, and then rfhSP-D (10, 5, 2.5 and 1.25µg/ml) was pre-incubated with pH1N1 or H3N2 virus (1.36×10^6pfu/ml) diluted in 200µl of PBS + 5mM $CaCl_2$; 10 µl of diluted virus was added to the corresponding wells, and incubated at RT for 2h. Maltose binding protein (MBP) was used as a negative control. The microtiter wells were then washed with PBS three times, and fixed with 4% Paraformaldehyde (PFA) (Fisher Scientific) for 10 minutes at RT. The wells were washed again with PBS three times, and blocked with 2% w/v BSA in PBS for 2 h at 37°C. Monoclonal anti-influenza virus H1 (BEI-Resources) and polyclonal anti-influenza virus H3 (BEI-Resources) in PBS (1:5000) were added to each well and incubated for 1h at 37°C. After washing with PBST three times, the corresponding wells were probed with goat anti-mouse IgG-HRP-conjugate (Thermo-Fisher), or Protein A-HRP conjugate (1:5000) in PBS for 1 h at 37ºC. The wells were washed again with PBST three times and the colour was developed using TMB substrate. The reaction was stopped using 2M H_2SO_4, followed by absorbance reading at 450nm.

Titration Assay

Maxisorp 96 well plates were coated with 0.01% collagen (Sigma-Aldrich) and incubated at RT for 3h. After removing the excess collagen, the wells were washed with PBS twice. 75, 000 A549 cells were seeded and grown overnight at 37°C in the presence of 5% v/v CO_2, until 75%-80% confluency. Cells were washed with 1 × PBS twice, pH1N1 or H3N2 virus (MOI of 1) diluted in pure DMEM with 10 µg/ml rfhSP-D was added to cells respectively. The plates were then incubated at 37°C incubator for 1 hour, and following post incubation, the wells were washed with PBS twice and 200µl of infectious medium was added to the cells, and incubated for 24h at 37°C with 5% v/v CO_2. The media of the infected cells in the presence and absence of rfhSP-D was collected and viral titre was estimated by $TCID_{50}$.

Infection assay using pH1N1 and H3N2

A549 cells were cultured in complete DMEM medium with usual supplements at 37ºC in CO_2 incubator until about 70-80% confluence. Cells, washed with PBS twice, trypsinised, and adjusted to 5 x 10^5 cells in 12 well plates (Fisher Scientific), were left to adhere overnight at 37ºC in serum free complete DMEM medium. Cells were washed in PBS before the addition of rfhSP-D (10µg /well) in pure DMEM containing 5mM $CaCl_2$ with MOI 1 of pH1N1 or H3N2 virus (1 h at RT and 1h at 4ºC). The pre-incubated virus and protein mix was then added onto the cells in a circular motion and incubated at 37ºC for 1 h in DMEM medium only. Medium containing unabsorbed virus and rfhSP-D protein was removed, cells were washed with PBS twice, infectious medium was added, and then left to incubate 2h and 6h. The infected cells were detached by scrapping with a sterile cell scrapper, centrifuged at 1500 ×g 3 minutes, and frozen at -80 ºC for further analysis via qPCR.

Real-time quantitative PCR analysis

The infected A549 cells were lysed using a lysis solution (50 mM Tris-HCl pH 7.5, 200 mM NaCl, 5 mM EDTA pH 8, 0.1% v/v Triton X-100). Total RNA was extracted using RNase Mini Kit (Qiagen). Contaminating DNA was removed by DNase I treatment, followed by heat-inactivation at 70°C of DNase I and RNase. A260nm was used to quantify the amount of RNA using NanoDrop 2000/2000c (Sigma-Aldrich) and the RNA purity was assessed using A260/A280 ratio between 1.8 and 2.1. The isolated RNA was then converted into cDNA using SuperScript II Reverse Transcriptase (Thermo-Fisher Scientific). Oligo-dT primers were added to initiate cDNA synthesis and to avoid labelling of the rRNA and tRNA. cDNA

was synthesized using high capacity RNA to cDNA Kit (Thermo-Fisher Scientific) using 1-2 µg of total RNA. Primer sequences were designed for specificity using the Primer-BLAST software (Basic Local Alignment Search Tool) (http://blast.ncbi.nlm.nih.gov/Blast.cgi) (Table 1). The qRT-PCR was performed using the Light Cycler system (Applied Biosciences). The amplification program used was at 95ºC for 5 min, followed by 45 cycles of 95ºC for 10 s, 60ºC for 10 s and 72ºC for 10 s. The specificity of the assay was established by melting-curve analysis.

Multiplex cytokine array analysis

Supernatant from A549 cells, incubated with IAV with and without rfhSP-D for 24h were collected for measuring secreted Cytokines (TNF-α, IL-6, IL-10, IL-1α, IFN-α and IL-12p40), chemokine (eotaxin) and growth factor (GM-CSF and VEGF). The analytes were measured using MagPixMilliplex kit (EMD Millipore). 25 µl of assay buffer was added to each well of a 96-well plate, followed by addition of 25 µl of standard, control or supernatant from A549 cells infected with pH1N1 or H3N2 (with and without rfhSP-D). 25 µl of magnetic beads, coupled to analytes, were added to each well, and incubated for 18 h at 4˚C. The plate was washed with the assay buffer and 25 µl of detection antibodies were incubated with the beads for 1h at RT. 25 µl of Streptavidin-Phycoerythrin was then added to each well and incubated for 30 mins at RT. Following a washing step, 150 µl of sheath fluid was added to each well and the plate was read using the Luminex Magpix instrument. Assays were conducted in duplicate.

Production of H1+N1 pseudotyped lentiviral particles

HEK293T cells were co-transfected with 20 µg of pcDNA3.1-swineH1-flag (H1 from swine H1N1 A/California/04/09) (Invitrogen), pcDNA3.1-swine N1-flag (N1 from swine H1N1 A/California/04/09) (Invitrogen), pHIV-Luciferase backbone (Addgene), which carries a modified proviral HIV-1 genome with *env* deleted and designed to express the firefly luciferase reporter, and psPAX2 (Addgene). psPAX2 is a second generation lentiviral packaging plasmid and can be used with second or third generation lentiviral vectors and envelope expressing plasmid. VSVG lentivirus was produced in a similar way as described above, replacing H1 + N1. Supernatant containing the released H1+N1 pseudotyped and VSVG lentiviral particles were harvested at 24h and 48h and centrifuged at 5000 ×g for 10 minutes to remove any debris, and concentrated via ultra-centrifugation. The transfected HEK 293T cells were lysed using lysis buffer (50 mM Tris-HCl pH 7.5, 200 mM NaCl, 5

mM EDTA, 0.1% v/v Triton X-100). The filtered supernatant and the cell lysate were analysed via western blotting and luciferase reporter activity assay.

Luciferase reporter activity assay

MDCK cells were cultured in supplemented DMEM medium as described earlier, until about 70-80% confluency. The harvested H1 + N1 pseudotyped particles at 24h and 48h were used to perform Luciferase reporter activity using luciferase one step assay kit (Thermo Scientific). rfhSP-D (5 and 10 µg/ml) was used to determine its effect on the Luciferase reporter activity; and cells only, and cells + H1+N1 particles were used as controls. Readings were measured using a GloMax 96 Microplate Luminometer (Promega).

Statistical Analysis

Graphs were generated using GraphPad Prism 6.0 software and the statistical analysis was performed using a two-way ANOVA test. Significant values were considered based on $*p < 0.1$, $**p < 0.05$, $***p < 0.01$, and $****p < 0.001$ between treated and un-treated conditions. Error bars show the SD or SEM, as indicated in the figure ligands.

Results

rfhSP-D binds directly to influenza A virus (IAV) strains

E.coli BL21 (λDE3) pLysS under bacteriophage T7 promoter containing the pUK-D1 construct (19), expressed a ~20 kDa protein following IPTG induction, compared to the un-induced bacterial cells (Figure 1A). The over-expressed insoluble rfhSP-D as inclusion bodies was refolded via denaturation and renaturation cycle. The soluble rfhSP-D fractions were affinity purified using maltose – agarose column, which appeared as a single band on 12% SDS-PAGE (v/v) under reducing condition (Figure 1B). The immunoreactivity of purified rfhSP-D was confirmed via western blotting, by using polyclonal anti- human SP-D antibody that was raised against native human SP-D purified from lung lavage of alveolar proteinosis patients (Figure 1C). The ability of pH1N1 and H3N2 strains to bind microtiter-coated rfhSP-D was examined via ELISA. As shown in Figure 2, rfhSP-D bound both IAV strains in a dose-dependent manner. VSVG lentivirus was used as a negative control RNA virus, where no significant binding was seen with all rfhSP-D concentration tested. For cell binding assay, A549 cells were challenged with purified pH1N1 or H3N2 MDCK pre-

incubated with rfhSP-D at different concentrations (Figure 3). The maximum inhibition of cell binding was seen at 10µg. MBP was used as a negative control protein.

rfhSP-D binds to HA and restricts replication of IAV in A549 cells

Previous studies have shown that SP-D binds to the glycosylation of HA1 domain on IAV (17). Far western blotting revealed that rfhSP-D bound to HA1 (55kDa) and HA2 (25kDA) of both pH1N1 (Figure 4A) and H3N2 (Figure 4B) strains. As show in figure 4C, rfhSP-D was able to bind purified recombinant HA protein in a concentration dependent manner. The binding of rfhSP-D may inhibit cellular viral infection by restricting the interaction of HA with sialic acid containing receptors, and HA-mediated fusion in endosomes. The interaction between rfhSP-D and HA appears to offer another dimension at which rfhSP-D may suppress target cell infection and intracellular replication. The mechanism of direct inhibition of IAV by rfhSP-D was thus investigated via infection assay. A549 cells infected with pH1N1 and H3N2 revealed an up-regulation of M1 expression at 2h and 6h time points (Figure 5). However, A549 cells, pre-treated with rfhSP-D showed down-regulated expression of viral M1 when compared to untreated cells challenged with virus (Figure 5). The down-regulation of M1 expression due to rfhSP-D pre-incubation was more effective in the case of pH1N1 compared to H3N2, where -8 $\log_{10}$ folds down-regulation was seen at 2 h (figure 5A). This was validated via western blotting, where a low M1 expression was detected in rfhSP-D (10 µg/ml) treated sample following 6h incubation, when compared to untreated samples (cells + virus) (Figure 5C). Furthermore, anti-IAV activity of rfhSP-D was confirmed via titration assay (Figure 5D and E). An approximate of 40% titre reduction was seen with 10µg rhfSP-D treated samples compared to untreated samples, suggesting the ability of rfhSP-D to act as an entry inhibitor by inhibiting the viral replication and viral titre. Differential inhibitory effects of rfhSP-D on IAV strains may reflect on the glycosylation of the HA protein of IAV, suggesting a correlation between HA-glycan attachment and susceptibility of IAV strains to inhibition by rfhSP-D that involves specific sites on the HA.

rfhSP-D modulates pro-inflammatory cytokine/chemokine immune responses following virus challenge to A549 cells

The qPCR analysis revealed that there was an up-regulation of pro-inflammatory cytokines TNF-α and IL-6 by H3N2 strain, which were brought down slightly by rfhSP-D at 2h (Figure 6A). However, both TNF-α and IL-6 in the case of pH1N1was found to be down-regulated considerably by rfhSP-D at 2h, which gradually recovered during 6h (Figure 6B). IL-6,

which is crucial for the resolution of IAV infection, acts by inducing neutrophils mediated viral clearance as well as preventing neutrophils from virus-induced pronounced lung damage or injury. An elevated level of IL-6 in lung and serum has been reported in patients infected with pH1N1 (20). TNF-α and IL-6 are the key contributors to IAV- mediated respiratory diseases and acute lung injury. In contrast, there was a broad level of down-regulation of IL-12 in the case of both IAV strains incubated with rfhSP-D, suggesting a likely reduction of Th1 response and suppression of IFN-γ production by $CD4^+$ T cells. Suppressed transcript levels RANTES (1 $\log_{10}$ fold) by rfhSP-D was observed at 2h treatment in the case of pH1N1. However, in the case of H3N2 strain, RANTES was downregulated by 0.5-fold ($\log_{10}$) (Figure 6B) at 2h following treatment with rfhSP-D compared to untreated A549 cells only. Furthermore, suppression of IFN-α and IFN-β were also seen with rfhSP-D treatment at both 2h and 6h time point (Figure 6C). Both of these type I IFN cytokines plays a crucial anti-viral role against IAV, and determine the rate of viral replication in the initial stage of infection. Suppression of type I IFN levels suggests the ability of rfhSP-D to reduce the rate of viral replication, thereby reducing the levels of INF produced by the innate immune system.

Multiplex cytokine array analysis reveals a differential ability of rfhSP-D to trigger a dramatic downregulation of some of the key pro-inflammatory cytokines and chemokines

To assess secretion of cytokines, chemokines and growth factors over a period of 24h post rfhSP-D treatment, a multiplex cytokine array was performed sing supernatants of the IAV challenged and rfhSP-D treated A549 cells. rfhSP-D induced a dramatic suppression of some of the key pro-inflammatory cytokines and chemokines in the virus infected A549 cells. In the case of pH1N1, TNF-α, IFN-α, IL-10, IL-12 (p40), VEGF, GM-CSF and eotaxin were considerably suppressed by rfhSP-D treatment at 24h (Figure 7A). However, these suppressive effects of IL-10, VEGF, eotaxin and IL-12 (p40) were not so evident in the case of H3N2 strain at the secreted protein level, with the exception of TNF-α, IFN-α, and GM-CSF (Figure 7). These data seem to suggest that the extent of immunomodulatory effect of SP-D on host cells can vary considerably in a strain-specific manner.

406 **rfhSP-D binds to H1+N1 pseudotyped lentivirus and reduces luciferase reporter activity**

407 H1+N1 pseudotyped lentiviral particles were produced as a safe strategy to study the
408 differential or combinatorial involvement of HA or NA viral glycoproteins in the recognition
409 and neutralisation of IAV by rfhSP-D. The production of lentiviral particles pseudotyped
410 with envelope proteins H1+N1 was carried out by co-transfecting HEK293T cells with
411 plasmid containing the coding sequence of the indicated H1+N1, pHIV-Luciferase backbone,
412 and psPAX2. Purified H1+N1 pseudotyped particles and cell lysate harvested at 24h and 48h
413 were analysed via western blotting, and the expression level of HA was determined using
414 anti-H1 monoclonal antibody (Figure 8A); HA was evident at 70kDa. Far western blotting
415 revealed binding of rfhSP-D to HA1 at 55kDa (Figure 8B), suggesting that the binding of
416 rfhSP-D to HA1 is crucial for the inhibition of viral infectivity. Purified H1+N1 pseudotyped
417 particles harvested at 24h and 48h were used to transduce MDCK cells to measure the
418 luciferase reporter activity assay. Higher levels of luciferase reporter activity were observed
419 at 24h when compared to 48h post transfection (Figure 8C). Thus, pseudo-particles harvested
420 at 24h were used to transduce MDCK cells with and without rfhSP-D (5 and 10 μg/ml)
421 (Figure 8D). Nearly 50% reduction of luciferase reporter activity was seen with 10 μg/ml of
422 rfhSP-D compared to cells challenged with H1+N1 pseudotyped particles. This suggested an
423 entry inhibitory role of rfhSP-D against IAV.

424 **Discussion**

425 Respiratory tract infection caused by IAV is associated with up to half million mortality rates
426 worldwide and 5 million cases of morbidity per year. A new swine-origin H1N1 IAV,
427 identified in April 2009, spread worldwide, and was officially declared pandemic in June
428 2009. There are concerns that H1N1 or H3N2 viruses reassort with existing H5N1 virus using
429 bird or pig as intermediate hosts, giving rise to more pathogenic IAV strains. Thus, it is
430 fundamentally important to understand molecular mechanisms of host's first line of defence
431 against IAV in order to design and develop novel and effective anti-IAV strategies. SP-D
432 expressed at the mucosal sites including lungs plays an important role during IAV infection
433 (21). SP-D has been shown to have a wide range of innate immune roles including
434 neutralization, agglutination, opsonisation and clearance of viruses including IAV. The
435 binding ability of rfhSP-D to HIV-1 gp120 was reported, primarily in a dose and calcium
436 dependent manner (22). Human SP-D has also been shown to bind IAV HA and NA, and
437 thereby, trigger inhibition of viral attachment and entry into the host cells (23). However, the

mechanism of direct inhibition of IAV and pseudotyped viral particles by SP-D and subsequent immune response is not fully understood. Therefore, this study was aimed at understanding the mechanisms through which SP-D play a crucial role in host response against IAV.

Using two different IAV strains- pH1N1 and H3N2, in this study, we have shown that the entry inhibitory capability of rfhSP-D is not limited to a particular strain. To identify the interaction of rfhSP-D with IAV viral proteins, protein-protein interaction studies were carried out via ELISA, cell binding assay and far western blot. The ELISA (Figure 2) and cell-binding assay (Figure 3) revealed the maximal binding of rfhSP-D to both pH1N1 and H3N2 IAV strains at 5µg/ml, and the maximum inhibition of cell binding was seen at 10µg/ml of rfhSP-D. Furthermore, binding ability of rfhSP-D to purified recombinant HA protein was revealed in a concentration, and calcium dependent manner (Figure 4C). rfhSP-D bound HA1 (55kDa) and HA2 (25kDa) (Figure 4), which are subunits of influenza hemagglutinin (HA). N-linked oligosaccharides found on the IAV envelope glycoproteins (HA and NA) are known to be recognised by the CRD region of SP-D. Thus, HA-exposed glycans differing in location and numbers between IAV strains may be responsible for this interaction. rfhSP-D is thus likely to inhibit IAV infection by preventing the HA interaction with sialic acid containing receptors. A reverse genetic approach has been used to analyse the role of N- glycosylation sites on the head of H1 in modulating sensitivity to SP-D *in vitro* and *in vivo* (24). It was found that HA Asn-144 was a critical factor in sensitivity to SP-D, neutralisation by mouse lung fluids and disease in mice (24).

We also examined the immune response of A549 lung epithelial cells following IAV challenge in the presence or absence of rfhSP-D, which can impact upon cellular infection and viral replication. Therefore, the ability of rfhSP-D to modulate viral replication as well as inflammatory immune response following IAV challenge was examined via infection assay, qPCR and multiplex cytokine array. The key aspect of host-pathogen interaction arising out of this study is the ability of rfhSP-D-bound pH1N1 and H3N2 to undergo supressed replication, as evident by the expression of M1 gene. M1 is a matrix protein of IAV that lies beneath the lipid layer and is the most abundant protein, which is essential for viral stability and integrity. Thus, it plays a critical role in recruitment and assembly of viral sites, nuclear export of viral ribonucleoprotein complexes (RNPs), and establishing the host components for viral budding (25). rfhSP-D suppressed the expression of M1 in pH1N1 (Figure 5A) at 2h, while down regulating at 6h in the case of H3N2 (Figure 5B). In addition, a lowered M1

expression was detected via western blot in the rfhSP-D treated sample compared to un-treated sample following 6h incubation (Figure 5C). Additionally, viral replication was also reduced in the presence of rfhSP-D as evident in figure 5. Thus, this suggest that rfhSP-D could act as an entry inhibitor of the strains tested (pH1N1 and H3N2). It is known that HA undergoes N-linked glycosylation and leads to modulation of antigenicity, fusion activity, receptor-binding specificity, and immune evasion of IAV. Therefore, SP-D can play an important role in innate defence against IAV as entry inhibitor by interfering with glycosylation sites and binding to glycans on the viral HA. It has been reported that the combinatorial substitutions of D325A/S+R343V in a trimeric neck and carbohydrate recognition domain fragment of human SP-D exhibits markedly increased anti-viral activity against pandemic IAV compared to native SP-D. This is because of the increased ability of the mutant to block the sialic acid binding sites, aggregate the virus and reduce viral uptake (26).

Our qPCR data demonstrated an increased expression level of TNF-α and IL-6 in H3N2 strain (Figure 6B) compared to pH1N1. However, when pH1N1 treated with rfhSP-D, TNF-α and IL-6 were suppressed at 2h (Figure 6A), which recovered towards the later stage of time point (6 h). Elevated mRNA expression levels of both TNF-α and IL-6 contribute to virus-mediated respiratory diseases or acute lung injury. IL-12 was considerably down-regulated by rfhSP-D in the case of both IAV strains, suggesting the likely suppression of Th1 immune response. mRNA expression of RANTES was 10-fold ($log_{10}1$ fold) down-regulated in the presence of rfhSP-D at 2h time point in pH1N1 compared to A549 cells only challenged with IAV. However, cells, challenged with H3N2 and treated with rfhSP-D, were seen to have log_{10} 1-fold down-regulation of RANTES expression. The role of type I interferon (IFN), including IFN-α and IFN-β, is established in host defence against IAV by clearing viral particles during the initial stage of infection. In this study, we report the ability of rfhSP-D (10 µg/ml) to downregulate both IFN-α and IFN-β expression (Figure 6C) at 2h and 6h incubation. A higher expression levels of both IFN-α and IFN-β was detected in untreated (cells virus) sample, whereas an approximate of 3-fold (log10 fold) downregulated in the presence of rfhSP-D following incubation at 6h. This suggest that when cells were incubated with either pH1N1/H3N3 (MOI 1), a higher levels of both IFN-α and IFN-β being produced by the immune system to clear the virions, while adding rfhSP-D has induced inhibition of viral replication, thus, a lower levels of INF was detected. Recently, the E3 ubiquitin ligase, TRIM29, has been shown to be a negative regulator of type I IFN responses in the lungs post-

IAV challenge *in vivo*. TRIM29 acts by inhibiting interferon-regulatory factors (IRFs) and signalling via NF-κB, leading to degradation of NF-κB Essential Modulator (NEMO) (27). Whether rfhSP-D works via similar mechanisms is worth further investigation using SP-D gene-deficient mice (28). In addition, cytokine array analysis using supernatants that were collected at 24h showed considerable downregulation of some of the key pro-inflammatory cytokines, chemokines and growth factors in the presence of rfhSP-D. The downregulation of various humoral factors by rfhSP-D treatment could also facilitate the prevention of life-threatening secondary bacterial infections that may be caused by aberrant virus-mediated immune modulations.

In this study, we have produced the second-generation lentiviral vectors pseudotyped for H1+N1 of IAV. This system contains a single packaging plasmid (psPAX2) encoding genes including Gag, Pol, and Tat. pHIV-Luciferase was used as a lentiviral transfer plasmid, which is flanked with long terminal repeat (LTR) sequences, and designed to express the firefly luciferase reporter. Thus, pHIV-Luciferase is 'replication incompetent' which contains an additional sequence deletion in the 3' LTR leading to viral 'self-inactivation' post integration. This method was selected as a safe alternative method to mimic the structure and surfaces of IAV, and to prove rfhSP-D as an entry inhibitor in MDCK cells transduced with pseudotyped IAV particles that are restricted to only one replicative cycle. The lentiviral particles pseudotyped with H1+N1 were analysed via SDS-PAGE and western blotting. Expression of HA in purified H1+N1 pseudotyped lentiviral particles from transfected HEK 293T cells was assessed by western blotting using anti-H1 monoclonal antibody (Figure 8A); HA appeared at 70kDa. H1+N1 pseudotyped lentiviral particles, purified via ultra-centrifugation, was used to investigate the combinatorial or differential involvement of viral envelope glycoproteins in the recognition and neutralization of HA particles by rfhSP-D. Incubation of rfhSP-D with these H1+N1 pseudotyped lentiviral particles was found to facilitate its binding to HA1 that appeared at 55kDA in the far western blot (Figure 8B). To validate the effectiveness of rfhSP-D as an entry inhibitor of IAV, luciferase reporter activity assay was performed. Nearly 50% luminescent signal was seen with 10 μg/ml of rfhSP-D when compared to MDCK cells challenged with H1+N1 pseudotyped lentiviral particles alone. This, therefore, suggested the ability of rfhSP-D to inhibit viral infectivity through binding to cell surface bound HA1 found on the infected MDCK cells.

In summary, suppression of M1 expression, pro-inflammatory cytokine response, as well as luciferase reporter activity in target cells by rfhSP-D highlights its potential as a therapeutic molecule in an entry inhibitory role against IAV.

References

(1) Nayak A, Dodagatta-Marri E, Tsolaki AG, Kishore U. An Insight into the Diverse Roles of Surfactant Proteins, SP-A and SP-D in Innate and Adaptive Immunity. *Front Immunol* (2012) 3:131. doi: 10.3389/fimmu.2012.00131 [doi].

(2) Crouch E, Hartshorn K, Horlacher T, McDonald B, Smith K, Cafarella T, et al. Recognition of mannosylated ligands and influenza A virus by human surfactant protein D: contributions of an extended site and residue 343. *Biochemistry* (2009) 48:3335-3345. doi: 10.1021/bi8022703 [doi].

(3) Hartshorn KL, Webby R, White MR, Tecle T, Pan C, Boucher S, et al. Role of viral hemagglutinin glycosylation in anti-influenza activities of recombinant surfactant protein D. *Respir Res* (2008) 9:65-9921-9-65. doi: 10.1186/1465-9921-9-65 [doi].

(4) Hartshorn KL, Crouch EC, White MR, Eggleton P, Tauber AI, Chang D, et al. Evidence for a protective role of pulmonary surfactant protein D (SP-D) against influenza A viruses. *J Clin Invest* (1994) 94:311-319. doi: 10.1172/JCI117323 [doi].

(5) Hartshorn KL, Sastry K, White MR, Anders EM, Super M, Ezekowitz RA, et al. Human mannose-binding protein functions as an opsonin for influenza A viruses. *J Clin Invest* (1993) 91:1414-1420. doi: 10.1172/JCI116345 [doi].

(6) Roberts KL, Manicassamy B, Lamb RA. Influenza A virus uses intercellular connections to spread to neighboring cells. *J Virol* (2015) 89:1537-1549. doi: 10.1128/JVI.03306-14 [doi].

(7) Mitnaul LJ, Matrosovich MN, Castrucci MR, Tuzikov AB, Bovin NV, Kobasa D, et al. Balanced hemagglutinin and neuraminidase activities are critical for efficient replication of influenza A virus. *J Virol* (2000) 74:6015-6020.

(8) Morens DM, Taubenberger JK, Harvey HA, Memoli MJ. The 1918 influenza pandemic: lessons for 2009 and the future. *Crit Care Med* (2010) 38:e10-20. doi: 10.1097/CCM.0b013e3181ceb25b [doi].

(9) Taubenberger JK, Morens DM. 1918 Influenza: the mother of all pandemics. *Emerg Infect Dis* (2006) 12:15-22. doi: 10.3201/eid1201.050979 [doi].

(10) Skehel JJ, Wiley DC. Receptor binding and membrane fusion in virus entry: the influenza hemagglutinin. *Annu Rev Biochem* (2000) 69:531-569. doi: 69/1/531 [pii].

(11) Wilson IA, Cox NJ. Structural basis of immune recognition of influenza virus hemagglutinin. *Annu Rev Immunol* (1990) 8:737-771. doi: 10.1146/annurev.iy.08.040190.003513 [doi].

(12) Glaser L, Stevens J, Zamarin D, Wilson IA, Garcia-Sastre A, Tumpey TM, et al. A single amino acid substitution in 1918 influenza virus hemagglutinin changes receptor binding specificity. *J Virol* (2005) 79:11533-11536. doi: 79/17/11533 [pii].

(13) Lakadamyali M, Rust MJ, Zhuang X. Ligands for clathrin-mediated endocytosis are differentially sorted into distinct populations of early endosomes. *Cell* (2006) 124:997-1009. doi: S0092-8674(06)00123-1 [pii].

(14) de Vries E, Tscherne DM, Wienholts MJ, Cobos-Jimenez V, Scholte F, Garcia-Sastre A, et al. Dissection of the influenza A virus endocytic routes reveals macropinocytosis as an alternative entry pathway. *PLoS Pathog* (2011) 7:e1001329. doi: 10.1371/journal.ppat.1001329 [doi].

(15) Stauffer S, Feng Y, Nebioglu F, Heilig R, Picotti P, Helenius A. Stepwise priming by acidic pH and a high K+ concentration is required for efficient uncoating of influenza A virus cores after penetration. *J Virol* (2014) 88:13029-13046. doi: 10.1128/JVI.01430-14 [doi].

(16) Tecle T, White MR, Crouch EC, Hartshorn KL. Inhibition of influenza viral neuraminidase activity by collectins. *Arch Virol* (2007) 152:1731-1742. doi: 10.1007/s00705-007-0983-4 [doi].

(17) Hartshorn KL, White MR, Voelker DR, Coburn J, Zaner K, Crouch EC. Mechanism of binding of surfactant protein D to influenza A viruses: importance of binding to haemagglutinin to antiviral activity. *Biochem J* (2000) 351 Pt 2:449-458.

(18) Hillaire ML, van Eijk M, Vogelzang-van Trierum SE, Fouchier RA, Osterhaus AD, Haagsman HP, et al. Recombinant porcine surfactant protein D inhibits influenza A virus replication ex vivo. *Virus Res* (2014) 181:22-26. doi: 10.1016/j.virusres.2013.12.032 [doi].

(19) Singh M, Madan T, Waters P, Parida SK, Sarma PU, Kishore U. Protective effects of a recombinant fragment of human surfactant protein D in a murine model of pulmonary hypersensitivity induced by dust mite allergens. *Immunol Lett* (2003) 86:299-307. doi: S0165247803000336 [pii].

(20) Paquette SG, Banner D, Zhao Z, Fang Y, Huang SS, Leomicronn AJ, et al. Interleukin-6 is a potential biomarker for severe pandemic H1N1 influenza A infection. *PLoS One* (2012) 7:e38214. doi: 10.1371/journal.pone.0038214 [doi].

(21) Ng WC, Tate MD, Brooks AG, Reading PC. Soluble host defense lectins in innate immunity to influenza virus. *J Biomed Biotechnol* (2012) 2012:732191. doi: 10.1155/2012/732191 [doi].

(22) Dodagatta-Marri E, Mitchell DA, Pandit H, Sonawani A, Murugaiah V, Idicula-Thomas S, et al. Protein-Protein Interaction between Surfactant Protein D and DC-SIGN via C-Type Lectin Domain Can Suppress HIV-1 Transfer. *Front Immunol* (2017) 8:834. doi: 10.3389/fimmu.2017.00834 [doi].

(23) Yang J, Li M, Shen X, Liu S. Influenza A virus entry inhibitors targeting the hemagglutinin. *Viruses* (2013) 5:352-373. doi: 10.3390/v5010352 [doi].

(24) Tate MD, Brooks AG, Reading PC. Specific sites of N-linked glycosylation on the hemagglutinin of H1N1 subtype influenza A virus determine sensitivity to inhibitors of the innate immune system and virulence in mice. *J Immunol* (2011) 187:1884-1894. doi: 10.4049/jimmunol.1100295 [doi].

(25) Rossman JS, Lamb RA. Influenza virus assembly and budding. *Virology* (2011) 411:229-236. doi: 10.1016/j.virol.2010.12.003 [doi].

(26) Nikolaidis NM, White MR, Allen K, Tripathi S, Qi L, McDonald B, et al. Mutations flanking the carbohydrate binding site of surfactant protein D confer antiviral activity for pandemic influenza A viruses. *Am J Physiol Lung Cell Mol Physiol* (2014) 306:L1036-44. doi: 10.1152/ajplung.00035.2014 [doi].

(27) Xing J, Weng L, Yuan B, Wang Z, Jia L, Jin R, Lu H, Li XC, Liu YJ, Zhang Z. Identification of a role for TRIM29 in the control of innate immunity in the respiratory tract. Nat Immunol. 2016 Dec;17(12):1373-1380. doi: 10.1038/ni.3580.

(28) Madan T, Reid KB, Singh M, Sarma PU, Kishore U. Susceptibility of mice genetically deficient in the surfactant protein (SP)-A or SP-D gene to pulmonary hypersensitivity induced by antigens and allergens of Aspergillus fumigatus. J Immunol. 2005 Jun 1;174(11):6943-54.

Table 1: Target Genes, Forward and Reverse primers used for qPCR

Target	Forward Primer	Reverse Primer
18S	5′-ATGGCCGTTCTTAGTTGGTG-3′	5′-CGCTGAGCCAGTCAGTGTAG-3′
IL-6	5′-GAAAGCAGCAAAGAGGCACT-3′	5′-TTTCACCAGGCAAGTCTCCT-3′
IL-12	5′-AACTTGCAGCTGAAGCCATT-3′	5′-GACCTGAACGCAGAATGTCA-3′
TNF-α	5′-AGCCCATGTTGTAGCAAACC-3′	5′-TGAGGTACAGGCCCTCTGAT-3′
M1	5′AAACATATGTCTGATAACGAAGGAGAA CAGTTCTT-3′	5′GCTGAATTCTACCTCATGGTCTTCTTGA-3′
RANTES	5'-GCGGGTACCATGAAGATCTCTG-3'	5'-GGGTCAGAATCAAGAAACCCTC-3'
IFN-α	5’-TTT CTC CTG CCT GAA GGA CAG-3’	5’-GCT CAT GAT TTC TGC TCT GAC A-3’
IFN-β	5’-AAA GAA GCA GCA ATT TTC AGC-3’	5’-CCT TGG CCT TCA GGT AAT GCA-3’

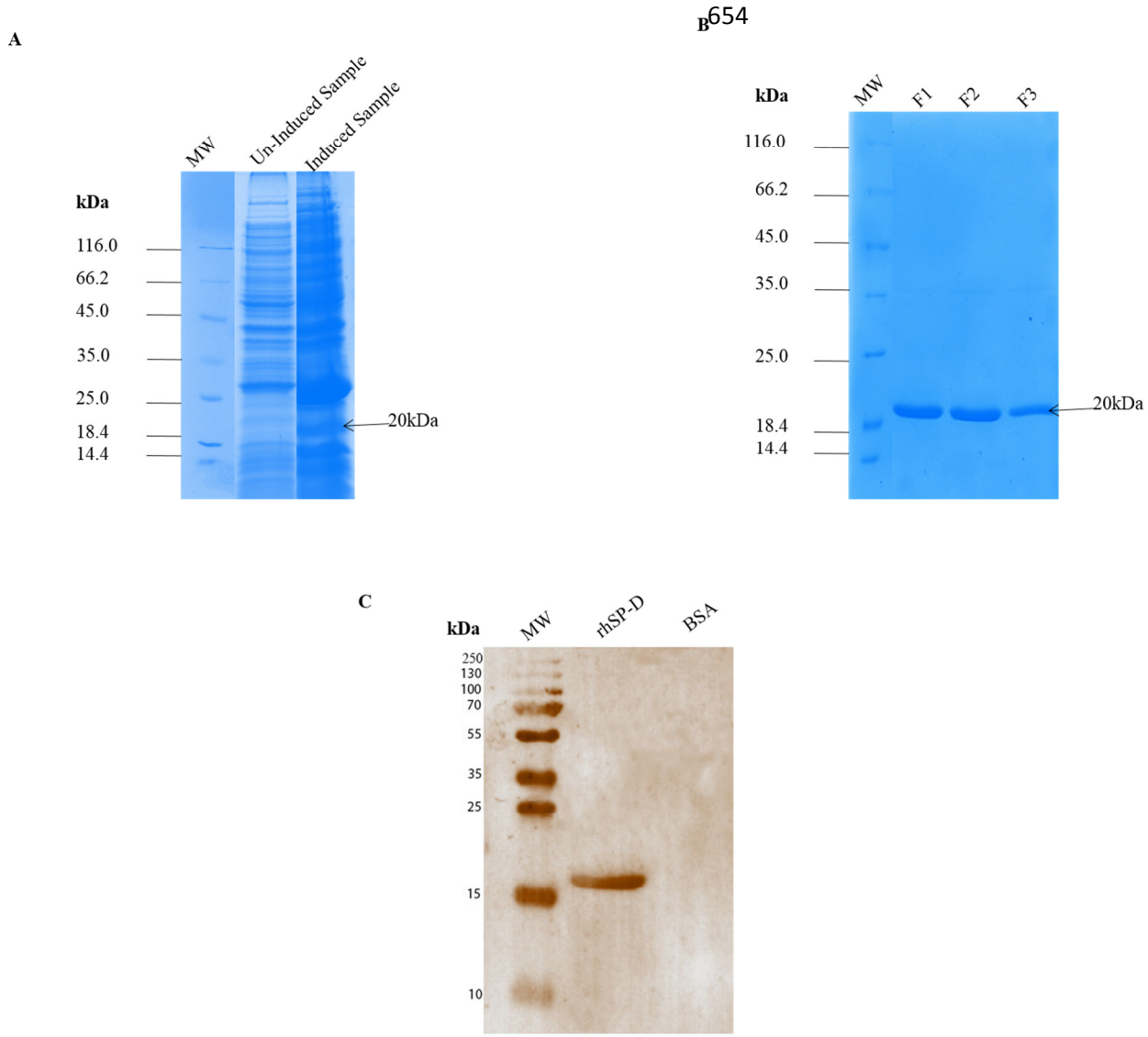

Figure 1: SDS-PAGE (12% v/v) under reducing conditions showing expression and purification of a recombinant surfactant protein D (rfhSP-D). The neck and CRD regions was expressed in *Escherichia coli* BL21 (λDE3) pLysS. (A) Following induction with 0.5mM IPTG, a ~20kDa band appeared being overexpressed compared to un-induced. Following denaturation-renaturation cycle, the rfhSP-D was purified on an affinity column to homogeneity (B). A rabbit polyclonal antibody raised against full length SP-D purified from Human bronchoalveolar lavage (C) recognised the purified rfhSP-D.

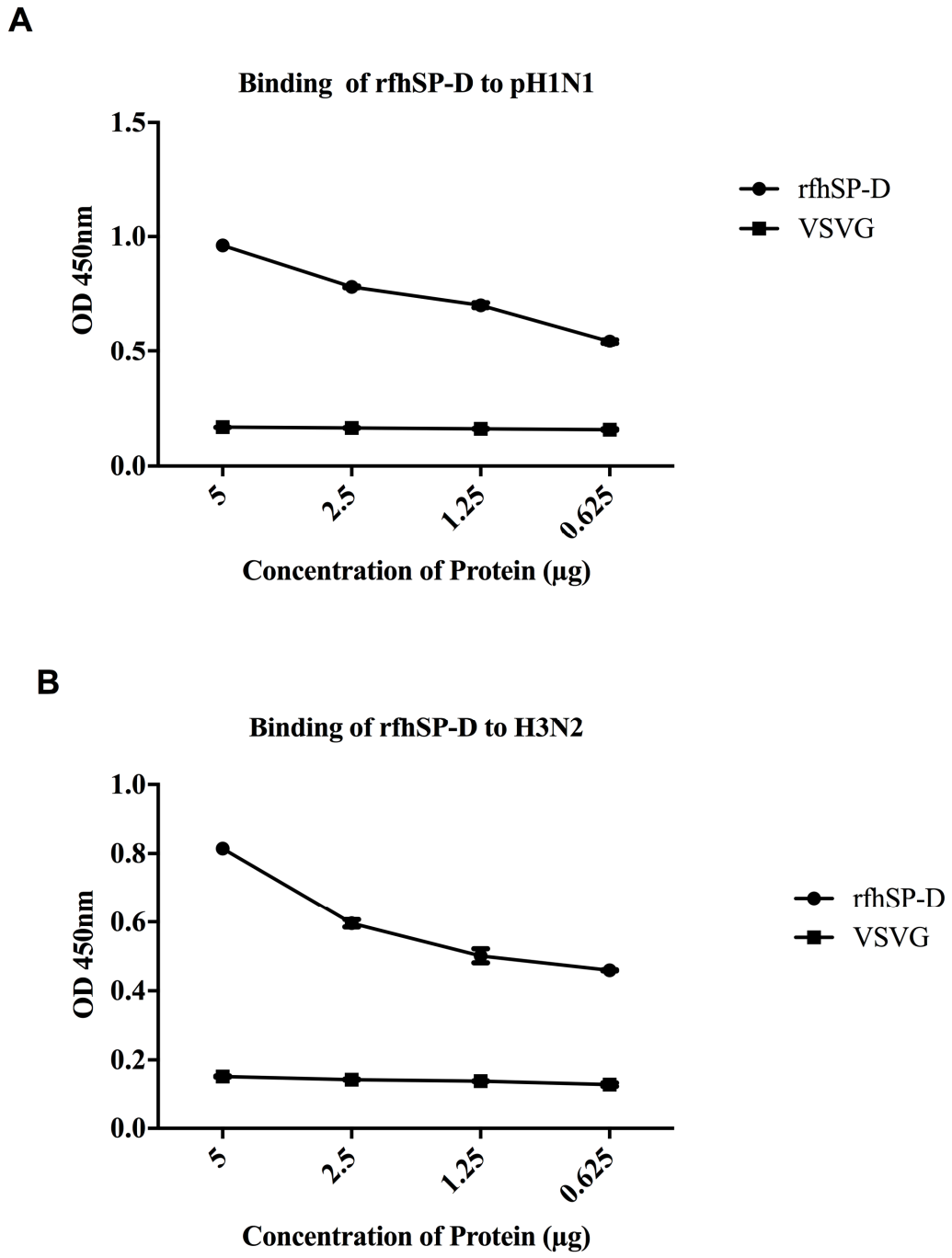

Figure 2: ELISA to show binding of rfhSP-D to (A) pH1N1 and (B) H3N2: Microtiter wells were coated with different concentration of rfhSP-D (5, 2.5, 1.25, and 0.625 µg/ml). 20 µl of concentrated pH1N1 or H3N2 virus (1.36×10^6pfu/ml) was diluted in 200µl of PBS + 5mM $CaCl_2$ and 10µl of diluted virus was added to all the wells, and probed with either monoclonal anti-influenza virus H1 or polyclonal anti-influenza virus H3 antibody. VSVG was used as a negative RNA virus control. The data were expressed as mean of three independent experiments done in triplicates ± SEM.

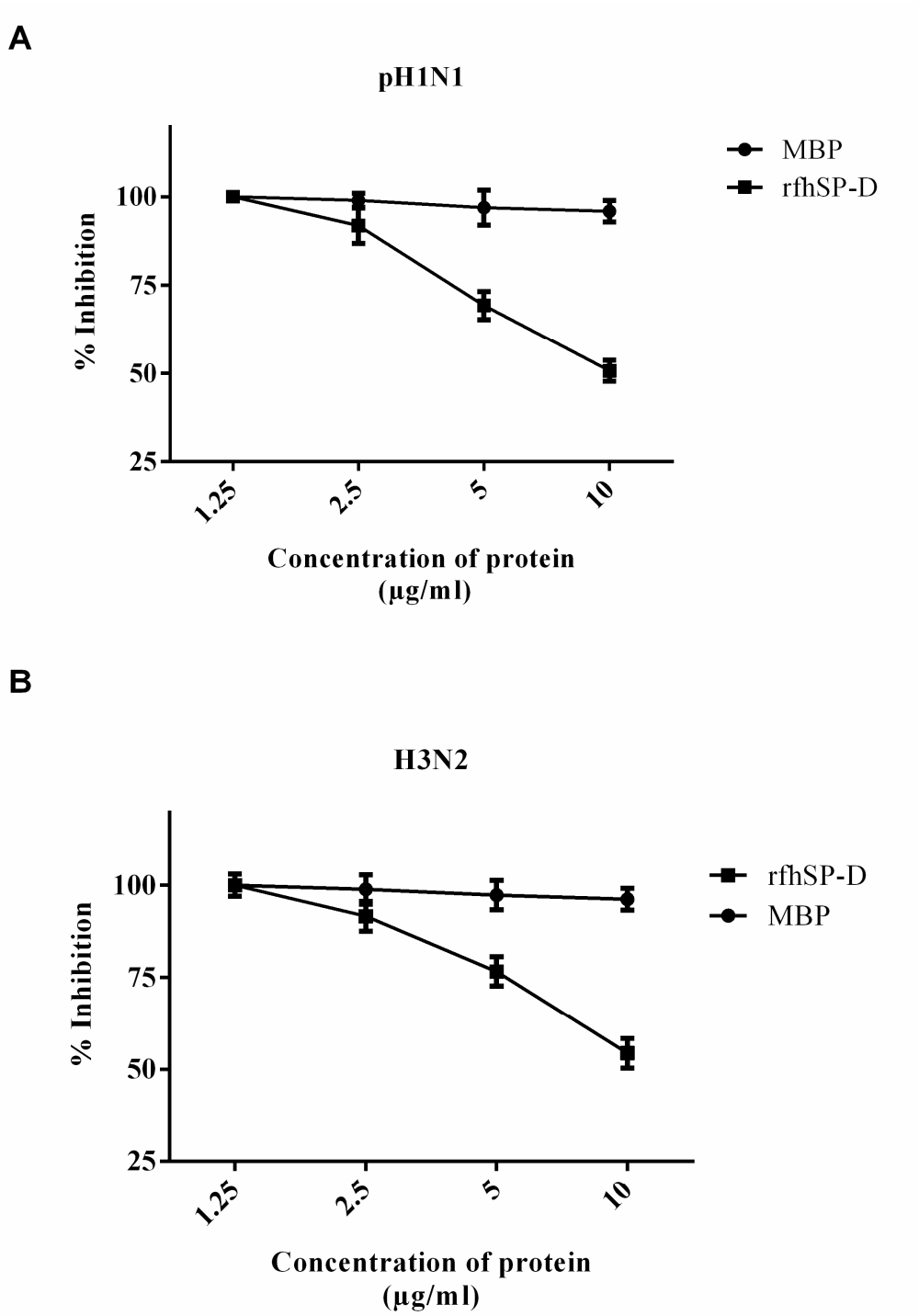

Figure 3: Cell Binding assay to show A549 cells binding to pre-incubated rfhSP-D with (A) pH1N1 and (B) H3N2. Microtiter wells were coated with A549 cells (1×10^5 cells/ml) and plates were incubated overnight at 37°C. Varied concentrations of pre-incubated rfhSP-D (10, 5, 2.5 and 1.25µg) with pH1N1/2009 and HK/99/H3N2 virus were added to the corresponding wells, followed by incubation at RT for 1-2 hours. After fixing, the cells with 4% Paraformaldehyde solution (PFA), monoclonal anti-influenza virus H1 and polyclonal anti-influenza virus H3 were added to each well. MBP was used as a negative control protein. The data were expressed as mean of three independent experiments done in triplicates ± SEM.

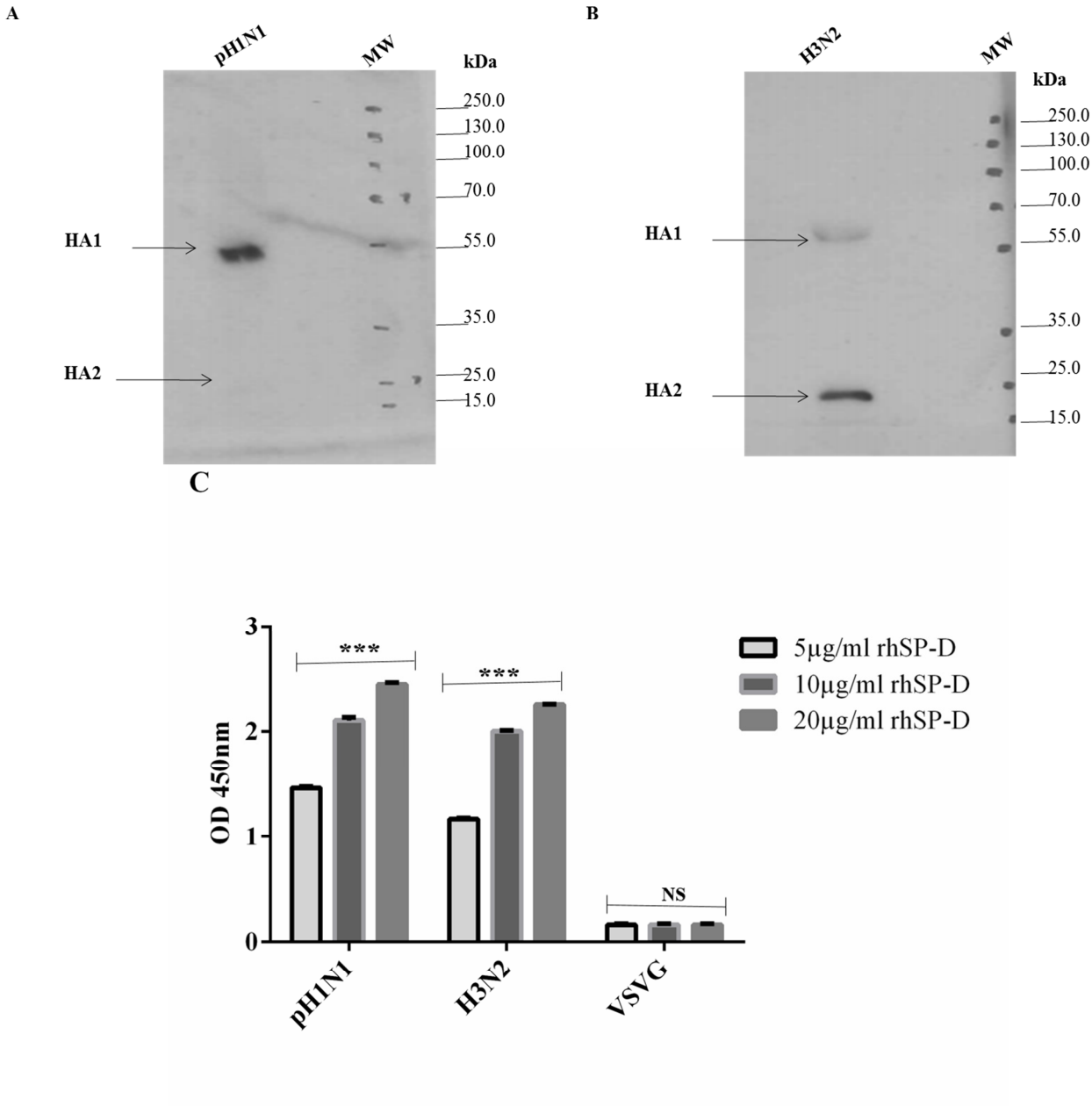

Figure 4: Far-western blot analysis to show rfhSP-D binding to purified (A) pH1N1 and (B) H3N2: 10 µ1 of concentrated virus (1.36×10^6 pfu/ml) was first run on the SDS-PAGE under reducing conditions, and then transferred onto a PDVF nitrocellulose membrane and incubated with 5µg of rfhSP-D. The membrane was probed with anti-rabbit SP-D polyclonal antibodies. rfhSP-D bound to HA1 (55kDa), and HA2 (25kDa) in the case of both pH1N1 and H3N2 strains. (C) ELISA to show the binding of rfhSP-D to purified recombinant hemagglutinin (HA) (µg/ml). VSVG was used as a negative control. The data were expressed as mean of three independent experiments carried out in triplicates ± SEM. Significance was determined using the unpaired one-way ANOVA test (*$p < 0.05$, **$p < 0.01$, and ***$p < 0.0001$) ($n = 3$).

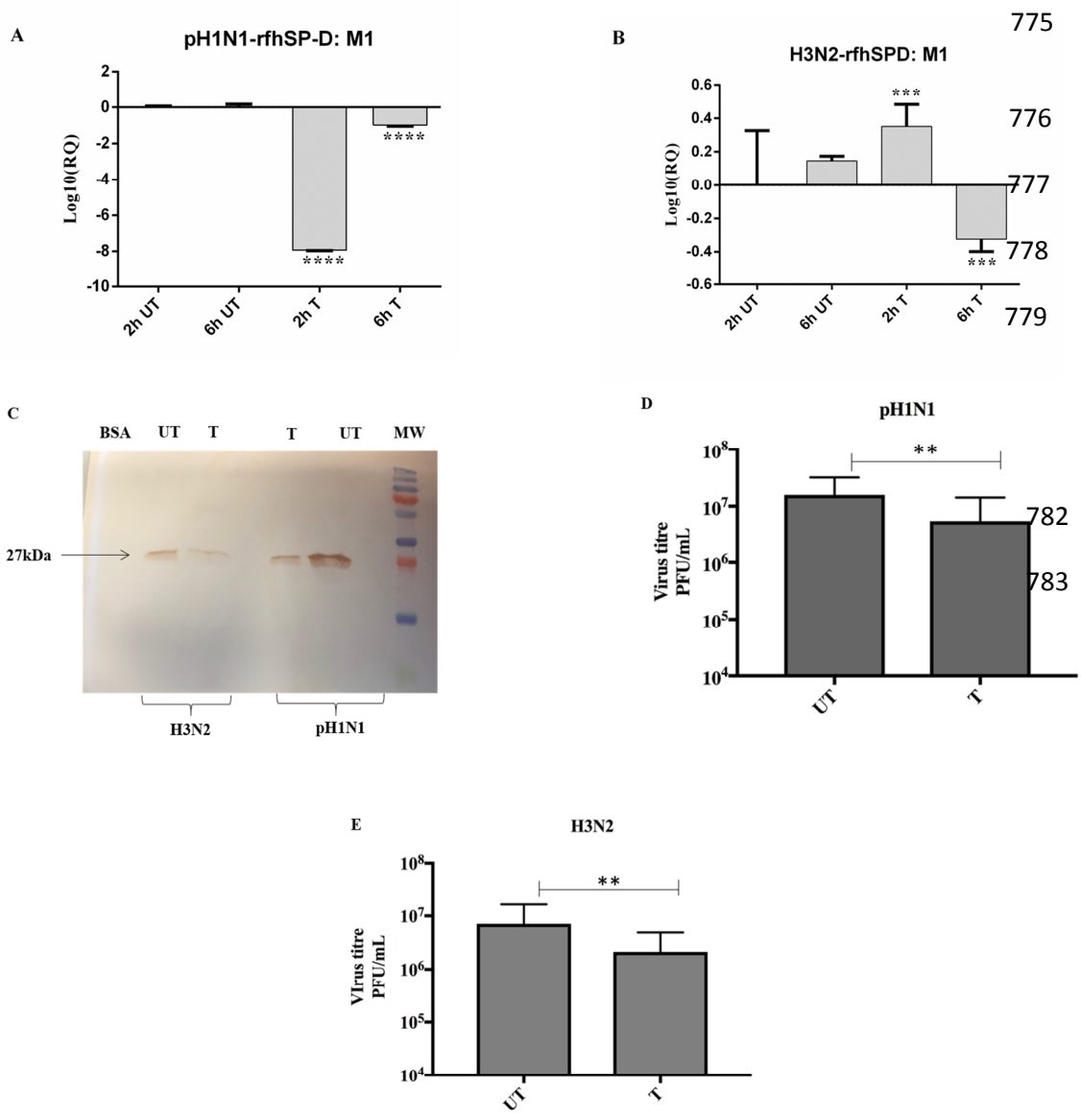

Figure 5: rfhSP-D restricts replication of (A) pH1N1and (B) H3N2 in target human A549 cells. M1 expression of both pH1N1 and H3N2 influenza A virus (IAV) (MOI 1) after infection of A549 cells at differential time points at 2h and 6 h. A549 cells were incubated either with pre-incubated pH1N1 and H3N2 with (10µg) or without purified rfhSP-D. Cell pellets were harvested at 2h and 6h to analyse the M1 expression of IAV. Cells were lysed, and purified RNA extracted was retro-transcribed into cDNAs. Infection was measured via qRT-PCR using M1 primers and 18S was used as an endogenous control. Results shown are normalised to M1 levels at 2 h untreated. Significance was determined using the unpaired one-way ANOVA test (*$p < 0.05$, **$p < 0.01$, and ***$p < 0.0001$) ($n = 3$). (C) Western blotting to shown M1 expression in both un-treated (cells + virus) and treated (cells + virus+10 µl/ml rfhSP-D) following 6h incubation. Titration assay to show the anti-IAV activity of rfhSP-D (10 µg/ml), suing both pH1N1 (D) and H3N2 (E) strains. A549 cells were infected with pH1N1/H3N2 (MOI 1) for 24 hours. Following post infection, the supernatants was collected and subjected to a TCID50 assay. An approximate of 40% reduction seen in titre in the treated samples, which suggests that rfhSP-D acts as an entry inhibitor.

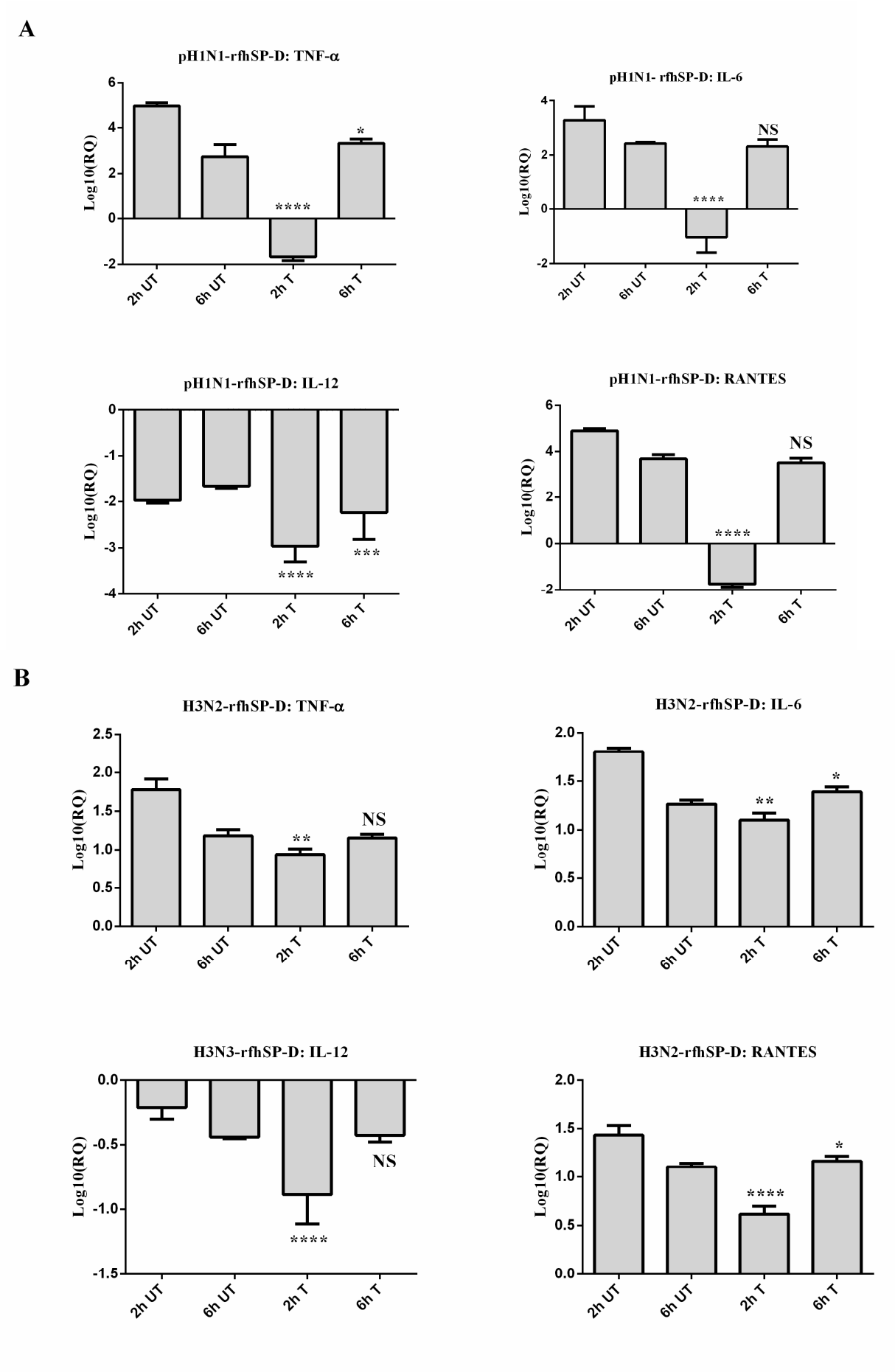
A
pH1N1-rfhSP-D: TNF-α
Log10(RQ)
6
4
2
0
-2
*
****
2h UT
6h UT
2h T
6h T
pH1N1- rfhSP-D: IL-6
Log10(RQ)
4
2
0
-2
NS
****
2h UT
6h UT
2h T
6h T
pH1N1-rfhSP-D: IL-12
Log10(RQ)
0
-1
-2
-3
-4
****
***
2h UT
6h UT
2h T
6h T
pH1N1-rfhSP-D: RANTES
Log10(RQ)
6
4
2
0
-2
NS
****
2h UT
6h UT
2h T
6h T
B
H3N2-rfhSP-D: TNF-α
Log10(RQ)
2.5
2.0
1.5
1.0
0.5
0.0
**
NS
2h UT
6h UT
2h T
6h T
H3N2-rfhSP-D: IL-6
Log10(RQ)
2.0
1.5
1.0
0.5
0.0
**
*
2h UT
6h UT
2h T
6h T
H3N3-rfhSP-D: IL-12
Log10(RQ)
0.0
-0.5
-1.0
-1.5
NS
****
2h UT
6h UT
2h T
6h T
H3N2-rfhSP-D: RANTES
Log10(RQ)
2.0
1.5
1.0
0.5
0.0
****
*
2h UT
6h UT
2h T
6h T

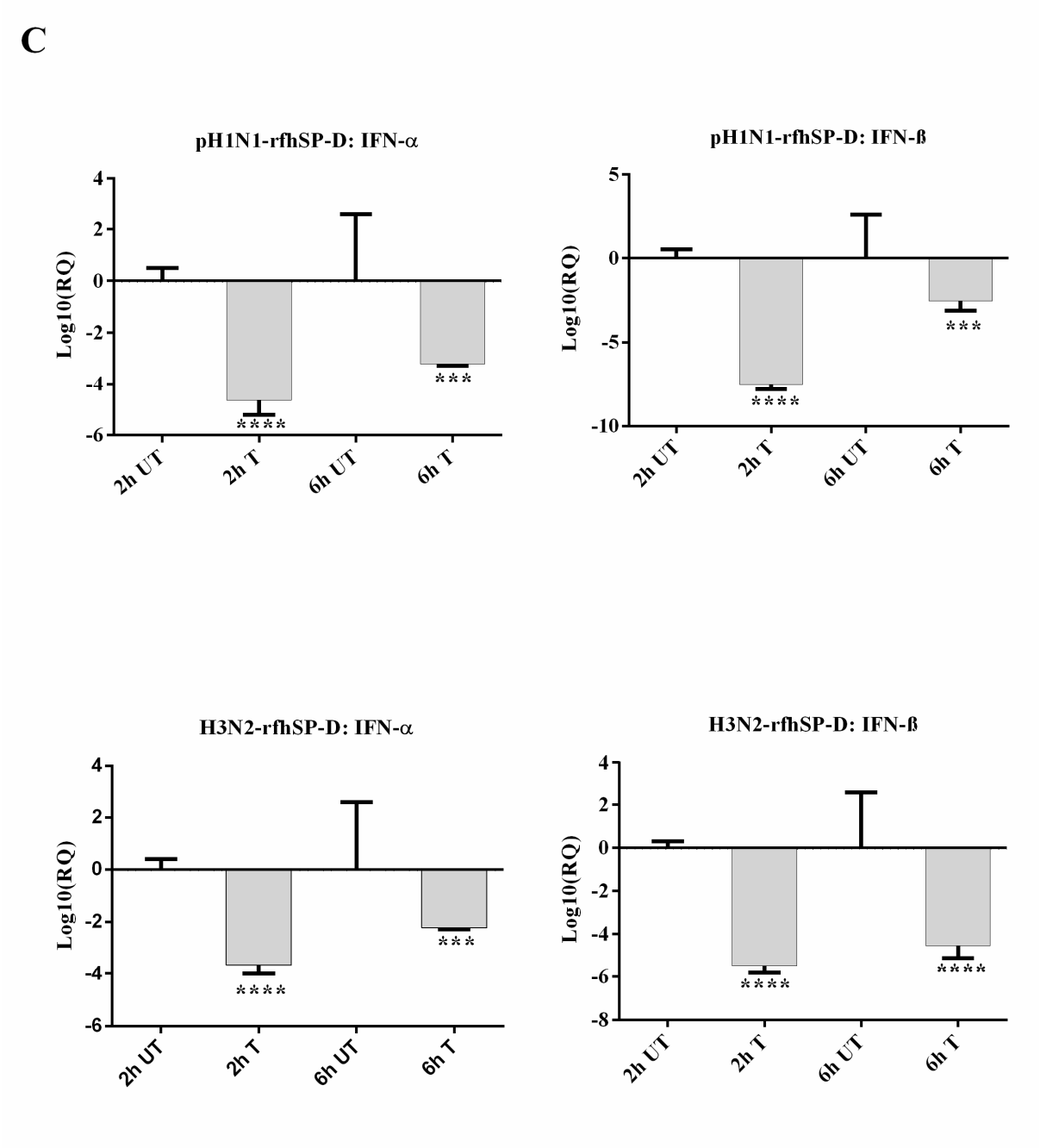

Figure 6: Differential mRNA expression profile of A549 cells challenged with pre-incubated (A) pH1N1, (B) H3N2 with rfhSP-D, and (C) expression levels of type I IFN subtypes in both untreated and treated samples. The expression levels of cytokines and Chemokine were measured using qRT-PCR and the data was normalised via 18S rRNA expression as a control. The relative expression (RQ) was calculated by using cells only time point as the calibrator. The RQ value was calculated using the formula: RQ = 2 $-\Delta\Delta$Ct. Assays were conducted in triplicates and error bars represents ±SEM. Significance was determined using the unpaired one-way ANOVA test (*$p < 0.05$, **$p < 0.01$, and ***$p < 0.0001$) ($n = 3$).

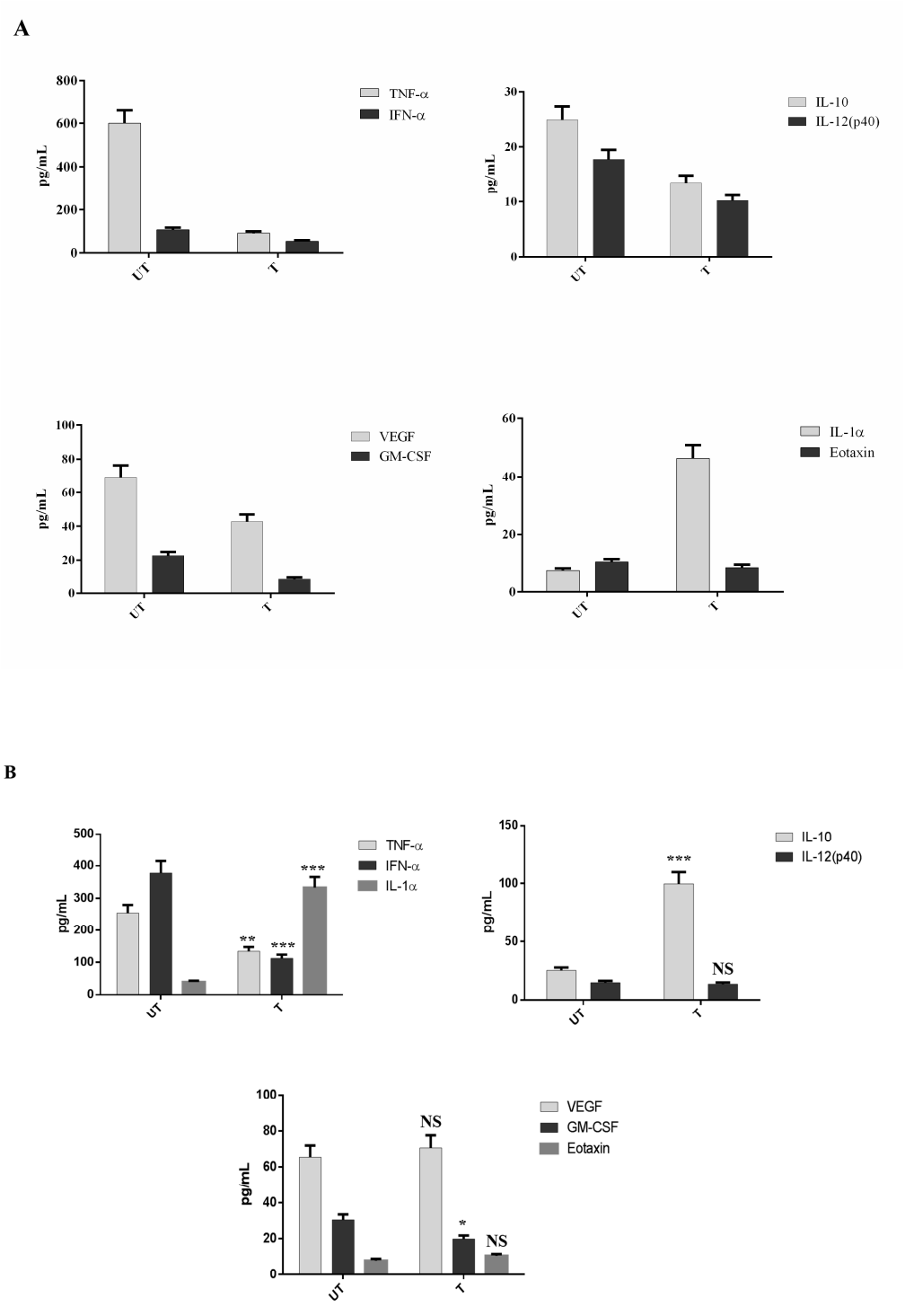

Figure 7: Multiplex cytokine array analysis of supernatants that were collected at 24 h time point. A549 cells were infected with pH1N1 (A) and H3N2 (B); treated with 10µg/ml of rfhSP-D. Cytokines (TNF-α IL-6, IL-10, IL-1α, IFN-α and IL-12p40), chemokine (eotaxin) and growth factor (GM-CSF, VEGF) concentrations were measured using a commercially available MagPix Milliplex kit (EMD Millipore). Assays were conducted in triplicates and error bars represents ±SEM (n=3).

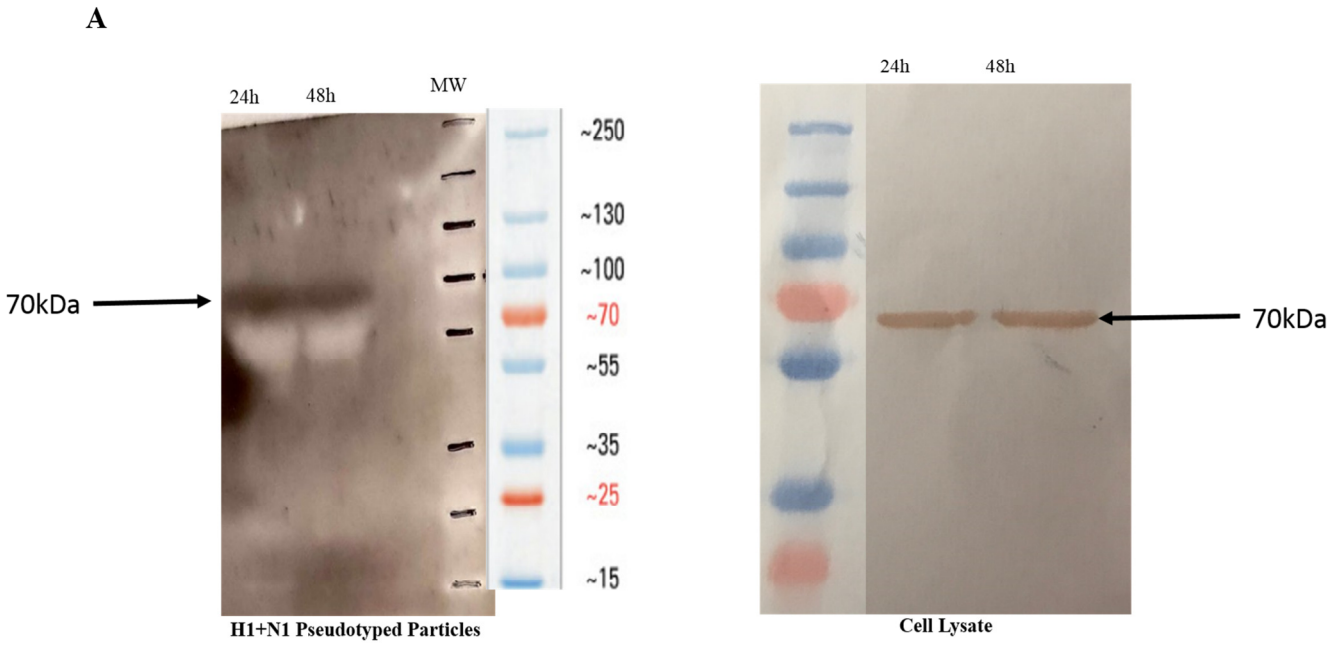
A
24h
48h
MW
~250
~130
~100
~70
~55
~35
~25
~15
70kDa
H1+N1 Pseudotyped Particles
24h
48h
70kDa
Cell Lysate

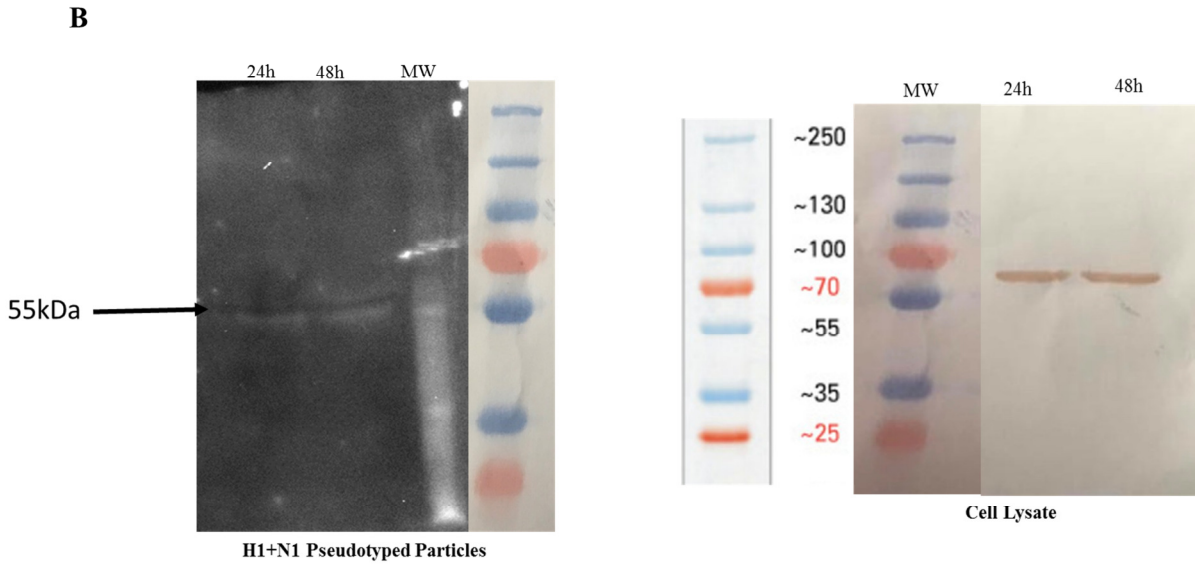
B
24h
48h
MW
55kDa
H1+N1 Pseudotyped Particles
MW
24h
48h
~250
~130
~100
~70
~55
~35
~25
Cell Lysate

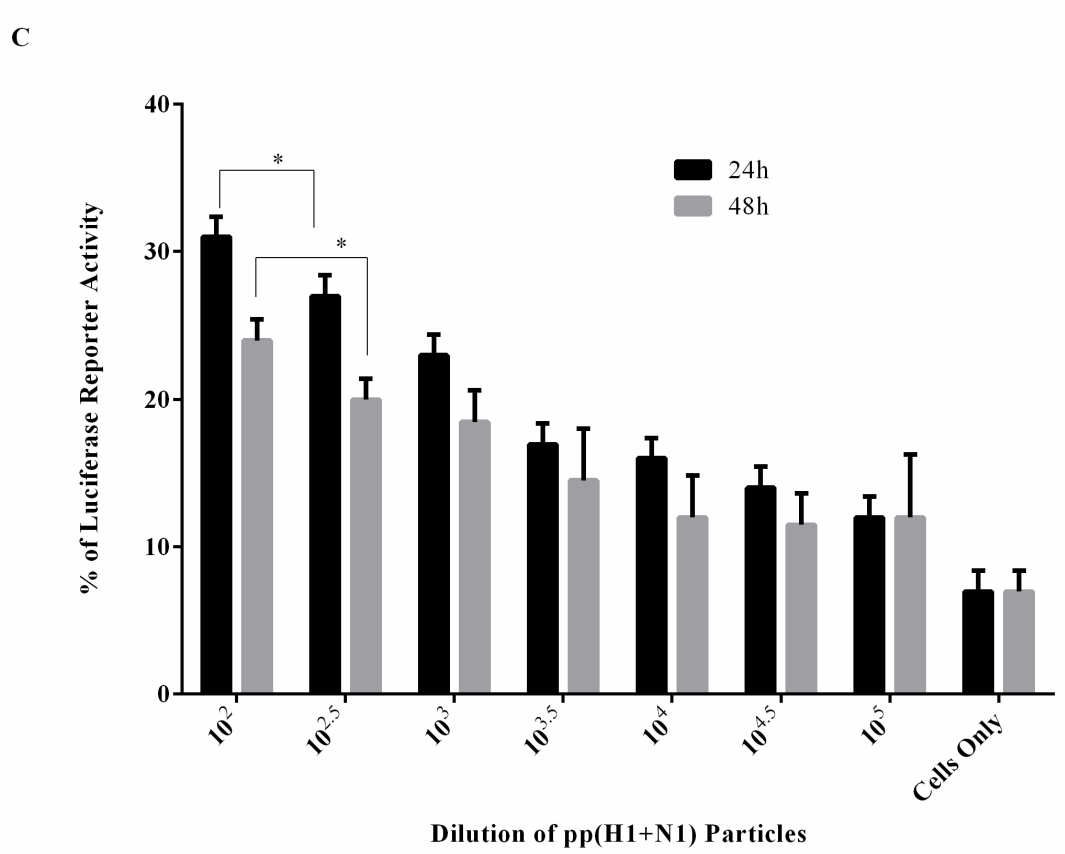
C
% of Luciferase Reporter Activity
40
30
20
10
0
*
*
24h
48h
10^2
10^2.5
10^3
10^3.5
10^4
10^4.5
10^5
Cells Only
Dilution of pp(H1+N1) Particles

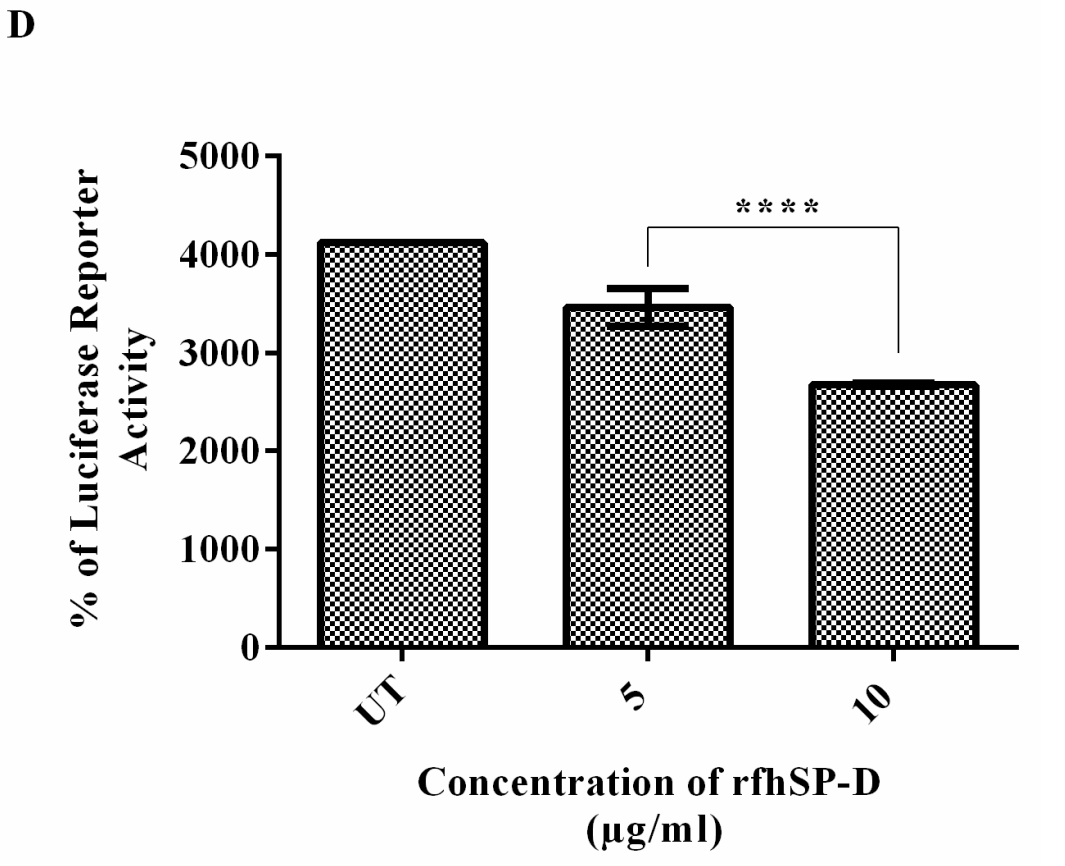
D
% of Luciferase Reporter Activity
5000
4000
3000
2000
1000
0
****
UT
5
10
Concentration of rfhSP-D (µg/ml)

Figure 8: (A) Western blotting to show the expression of IAV-HA protein in purified H1+N1 pseudotyped lentiviral particles and cell lysate at 24h and 48h. The presence of HA was identified at 70kDa. (B) far-western blotting to show rfhSP-D binding in both purified H1+N1 pseudotyped lentiviral particles and cell lysate at 24h and 48h. HA1 monomer was evident at 55 kDa when incubated with rfhSP-D. (C) Luciferase reporter activity of purified H1+N1 pseudotyped lentiviral particles at 24h and 48h, and (D) Luciferase reporter activity of rfhSP-D treated MDCK cells transduced with these lentiviral particles. Significance was determined using the unpaired one-way ANOVA test (*$p < 0.05$, **$p < 0.01$, ***$p < 0.001$and ****$p < 0.0001$) ($n = 3$).